

A radio minihalo in the extreme cool-core galaxy cluster RXCJ1504.1–0248

S. Giacintucci^{1,2}, M. Markevitch², G. Brunetti¹, R. Cassano^{2,3}, and T. Venturi¹

¹ INAF- Istituto di Radioastronomia, via Gobetti 101, I-40129, Bologna, Italy

² Harvard-Smithsonian Centre for Astrophysics, 60 Garden Street, Cambridge, MA 02138, USA,

³ Dip. Astronomia, University of Bologna, via Ranzani 1, I-40127 Bologna, Italy

Preprint online version: November 16, 2010

ABSTRACT

Aims. We report the discovery of a radio minihalo in RXCJ1504.1-0248, a massive galaxy cluster that has an extremely luminous cool core. To date, only 9 radio minihalos are known, thus the discovery of a new one, in one of the most luminous cool-core clusters, provides important information on this peculiar class of sources and sheds light on their origin.

Methods. The diffuse radio source is detected using GMRT at 327 MHz and confirmed by pointed VLA data at 1.46 GHz. The minihalo has a radius of ~ 140 kpc. A Chandra gas temperature map shows that the minihalo emission fills the cluster cool core and has some morphological similarities to it, as has been previously observed for other minihalos.

Results. The Chandra data reveal two subtle cold fronts in the cool core, likely created by sloshing of the core gas, as observed in most cool-core clusters. Following previous work, we speculate that the origin of the minihalo is related to sloshing. Sloshing may result in particle acceleration by generating turbulence and/or amplifying the magnetic field in the cool core, leading to the formation of a minihalo.

Key words. radiation mechanism: non-thermal – galaxies: clusters: general – galaxies: clusters: individual: RXC J1504.1–0248

1. Introduction

In some relaxed, cool-core clusters, the central radio galaxy is surrounded by diffuse radio emission with $\lesssim 150$ -300 kpc radius, with steep radio spectra ($\alpha > 1$; $S_\nu \propto \nu^{-\alpha}$, where S_ν is the flux density at the frequency ν) and low-surface brightness. These sources are roundish in shape and very different from the lobes of the radio galaxies often observed at the centre of cool-core clusters. They are classified as radio minihalos (e.g., Ferrari et al. 2008). Minihalos are rare; only nine cases have been detected so far (e.g., Burns et al. 1992; Bacchi et al. 2003; Venturi et al. 2007; Gitti et al. 2007; Govoni et al. 2009). Their physical properties and origin are still poorly known.

Minihalos cannot be explained by diffusion of relativistic electrons from the central galaxy, because the radiative lifetime of the electrons ($\sim 10^8$ yrs) is much shorter than the time needed for them to diffuse from the galaxy to the minihalo radius. A possibility is given by reacceleration of pre-existing, relativistic electrons in the intracluster medium (ICM) by turbulence in the cooling flow (Gitti et al. 2002). Buoyant bubbles of relativistic plasma, inflated by the central AGN and disrupted by the ICM motion, may provide the seed relativistic electrons that rapidly cool to energies where they do not emit in observable radio band. Thus, minihalos may be the ultimate depository of the relativistic matter ejected by the AGN over the cluster lifetime. However, the strong gas inflows caused by the cooling appear unlikely with the present understanding of cooling flows (e.g., Peterson & Fabian 2006). Thus, the origin of the turbulence needed to reaccelerate the electrons in minihalos is unclear. An interesting possibility is that it results from sloshing of the core gas, frequently observed in the X-ray (e.g., Markevitch & Vikhlinin 2007). This was hinted at by the discovery of a connection between minihalos and the sloshing cold fronts in two clusters (Mazzotta &

Giacintucci 2008). The minihalos appear confined within these fronts, and the radio emission is spatially correlated with the spiral structure of the fronts. Thus, old relativistic electrons injected over time by the central AGN may be spread out by gas sloshing and reaccelerated by turbulence generated by this sloshing. Spiral flows associated with sloshing may also amplify the magnetic fields at the fronts (Keshet et al. 2010), which may amplify the synchrotron emission. Hadronic collisions between thermal and cosmic ray protons can be alternative or additional sources for seed relativistic electrons (e.g., Pfrommer & Ensslin 2004).

In this Letter, we report the discovery of a radio minihalo at the centre of the massive, cool-core cluster RXCJ1504.1-0248 (hereafter RXCJ1504) at $z=0.215$ using archival *Giant Metrewave Radio Telescope* (GMRT) data and 1.46 GHz observations from the *Very Large Array* (VLA) archive. The cluster exhibits extreme characteristics. With a total X-ray mass of $1.8 \times 10^{15} M_\odot$ within a radius of 3 Mpc and a bolometric luminosity $L_{bol} = 4.3 \times 10^{45}$ erg s^{-1} , this system is one of the most luminous clusters known (Böhringer et al. 2005). Its global X-ray temperature is 10.5 keV. The overall X-ray morphology is very compact and relaxed, with a bright cool core with a cooling radius of ~ 140 kpc, in which the temperature drops below 5 keV. This extreme cool core accounts for more than 70% of the cluster total X-ray luminosity, making it one of the most luminous cool cores known (Böhringer et al. 2005).

We adopt $H_0=70$ km s^{-1} Mpc $^{-1}$, $\Omega_m = 0.3$ and $\Omega_\Lambda = 0.7$. At the redshift of RXC J1504 ($z=0.215$), this gives $1'' = 3.49$ kpc.

2. Chandra data reduction

We used archival *Chandra* data (ObsID 5793, ignoring another much shorter observation in the archive) to obtain the

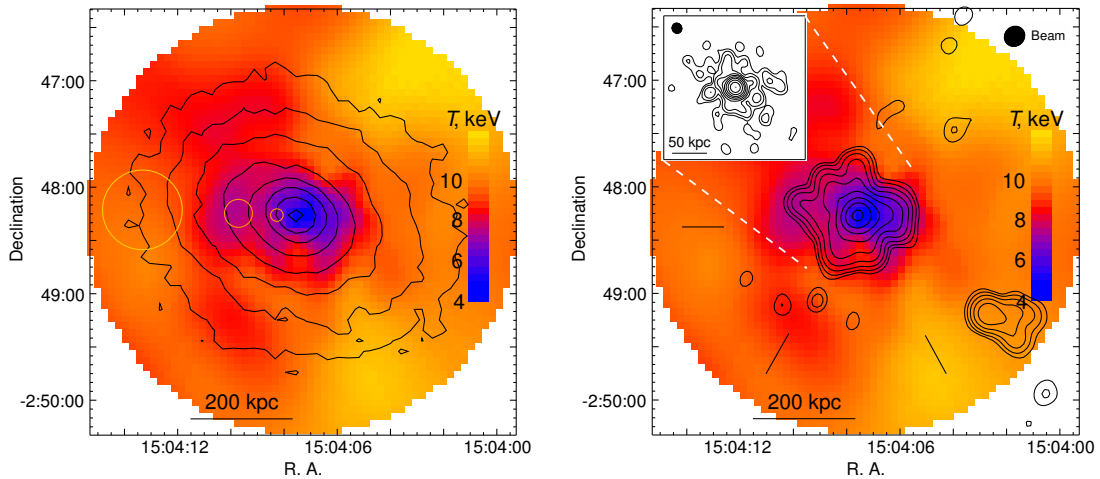


Fig. 1. *Left:* *Chandra* gas temperature map (color); contours overlay the 0.8–4 keV *Chandra* X-ray image smoothed with a $\sigma = 2''$ Gaussian. Contours are spaced by a factor of 2 in surface brightness. The radii of three circles illustrate the variable smoothing width (Gaussian σ) used for the temperature map. The rms temperature uncertainties at their positions (from small to large radius) are 0.3 keV, 0.5 keV and 0.9 keV. *Right:* *GMRT* 327 MHz contours of the minihalo overlaid on the gas temperature map. The radio beam is $11.3'' \times 10.4''$. Contours are spaced by a factor of 2, starting from $+3\sigma = 0.3 \text{ mJy beam}^{-1}$. Dashes show sectors used for radial profiles (Fig. 2). *Inset:* *VLA* 1.46 GHz pointed-observation image at resolution $4'' \times 4''$. Contours start at $0.1 \text{ mJy beam}^{-1}$ and scale by factor of 2. Black ellipses show beam sizes of the two radio images.

X-ray image and temperature map of the central region of RXCJ1504. The observation was performed with ACIS-I with ~ 40 ksec exposure. We cleaned the data and modelled the detector background and instrumental spatial response as described in Vikhlinin et al. (2005), using the latest *Chandra* calibration (CalDB 4.3.0). The temperature map was derived as described in Markevitch et al. (2000). Given the extremely bright cool core, we removed the ACIS readout artifact following Markevitch et al. (2000). We excluded point sources, produced background-subtracted and exposure-corrected images in several energy bands (0.8–1.2–2.2–3.0–4.5–6.5–9.0 keV) and then smoothed them by a Gaussian filter with the width dependent on the radius from the brightness peak, in order to get good angular resolution at the peak and good signal to noise ratio outside. A temperature in each pixel of the map was obtained by fitting values for each pixel of these images with a thermal plasma model, with N_H fixed to the Galactic value ($6 \times 10^{20} \text{ cm}^{-2}$) and the metal abundance to 0.4 solar (an average value for a fit to the central $r = 2'$ region). The resulting temperature map in the central $r = 2'$ is shown in Fig. 1 with X-ray contours overlaid (left). The map clearly shows the cool core, where the temperature of the gas drops to ~ 4 keV. The size of the cool core agrees with the estimate of the cooling radius (~ 140 kpc) by Böhringer et al. (2005). The eastern and western elongations of the cool core are significant at more than 2σ .

3. Radio observations and data reduction

RXCJ1504 was observed with the *GMRT* at 327 MHz as part of the *GMRT* Cluster Key Project (05VKK01). Table 1 summarizes the details of the observation: frequency, bandwidth, date, time on source, synthesized Full-Width Half-Maximum (FWHM) and position angle (PA) of the full array, rms level (1σ) at full resolution, and u-v range. The data were collected using the default spectral-line mode. Both upper and lower side bands (USB and LSB) were used, providing a total observing bandwidth of 32 MHz. We calibrated the USB and LSB datasets individually using the NRAO Astronomical Image Processing System (AIPS)

package, following the procedure described in Giacintucci et al. (2008). After bandpass calibration and a priori amplitude calibration, a number of phase-only self-calibration cycles and imaging were carried out for each data set. Multi-field imaging was implemented in each step of the data reduction. The USB and LSB data sets were then combined together to produce the final image, which has a noise of $100 \mu\text{Jy beam}^{-1}$ (Table 1).

We retrieved from the *VLA* archive the 1.46 GHz observation of RXCJ1504 in B-array configuration (see Table 1 for details). Calibration and data reduction were carried out in AIPS following the standard procedure (Fourier-transform, Clean and Restore). Phase-only self-calibration was applied to remove residual phase variations. The final image has a noise of $35 \mu\text{Jy beam}^{-1}$ (Table 1). Average residual amplitude errors in the data are $\lesssim 5\%$ both at 327 MHz and 1.46 GHz.

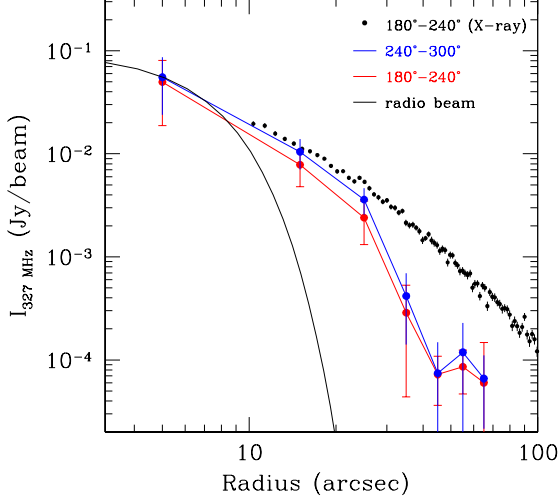
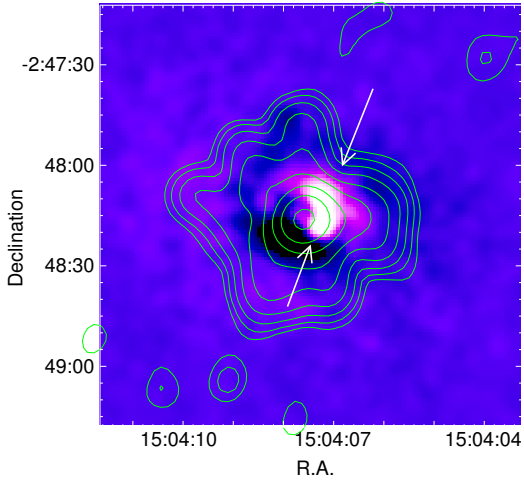
4. The minihalo and the cool core

In Fig. 1 (right), we overlay the *GMRT* 327 MHz contours on the temperature map. The central, unresolved radio component is associated with the elliptical galaxy at the cluster center. The diffuse minihalo surrounds this radio galaxy, extending for $\sim 40''$ (~ 140 kpc) in radius. The *VLA* $4''$ -resolution image at 1.46 GHz is presented in the inset. The image shows diffuse emission on a slightly smaller scale than the 327 MHz image (as expected for an interferometric image with a higher resolution), while resolving more details near the central compact source. No clear radio structures, such as jets or tails, connect the point source to the diffuse component, confirming that the emission seen in the *GMRT* image is indeed a minihalo.

Fig. 1 shows that the minihalo is mostly confined within the cool core. Some spatial radio features even coincide with similar structures of cool gas in the temperature map. To verify this, we produced 327 MHz images with lower resolution (not shown here) and found that the diffuse emission is indeed confined within those radii. Since the largest detectable structure provided by the *GMRT* at 327 MHz is $\sim 30'$, compared to the $\sim 1.3'$ size of the minihalo, we are confident that we are not

Table 1. Details of the radio observations of RXC J1504.1–0248

Telescope	Project	Frequency (MHz)	Bandwidth (MHz)	Observation date	Integration time (min)	FWHM, PA (full array, "x", °)	rms ($\mu\text{Jy b}^{-1}$)	u-v range (kl)
GMRT	05VKK01	327	32	2004 Apr 25	75	11.3×10.4, -44	100	~ 0.1 – 26
VLA–B	AM938	1465	50	2009 Apr 6	160	4.26×3.98, 29	35	~ 0.8 – 55


Fig. 2. 327 MHz brightness profiles (blue and red) extracted in sectors shown in Fig. 1 (right), centered on the radio peak. Comparison with the radio beam (black curve) clearly shows that the minihalo emission is extended. Black dots show the X-ray brightness profile in the same combined sector.

Fig. 3. A smoothed image of X-ray brightness residuals remaining after the subtraction of the best-fit elliptical β -model from the *Chandra* image of the core region. Two X-ray cold fronts are marked with arrows. Radio contours at 327 MHz are also shown (same as Fig. 1).

missing emission on a larger scale. Thus, the strong drop of the radio brightness at the minihalo boundary is real. Fig. 2 shows radial profiles of the radio emission extracted in two sectors in the south-east region of the core (shown by black dashes in Fig. 1). For comparison, we also show the X-ray brightness profile extracted in the same combined sector (black dots). There is an

abrupt drop in radio brightness at a radius $r > 25''$, while the X-ray profile continues smoothly beyond.

The 327 MHz flux density of the entire radio emission at the cluster center is $S_{327\text{MHz}} = 215 \pm 11$ mJy. The flux of the compact source (obtained from a Gaussian fit in the full resolution image) accounts for $\sim 44\%$ of the total flux, leaving 121 ± 6 mJy to the minihalo. The system is unresolved at the $45''$ -resolution of the 1.4 GHz NRAO VLA Sky Survey (NVSS) image, where a total flux of 62 mJy is measured. From the VLA image in the inset of Fig. 1, the contribution of the central compact source at 1.4 GHz is 42 ± 2 mJy. Subtracting this from the NVSS total flux, the 1.4 GHz flux density of the minihalo is 20 ± 1 mJy. The corresponding radio power is $P_{1.4\text{GHz}} = 3 \times 10^{24} \text{ W Hz}^{-1}$. Using the fluxes at 327 MHz and 1.4 GHz, the spectral index of the minihalo is $\alpha^1 = 1.24$, i.e., steep as typical for minihalos (e.g., Ferrari et al. 2008). The central point source has a flatter spectrum ($\alpha = 0.56$). The different $u-v$ coverage of the 327 MHz and 1.4 GHz data sets at short baselines (Table 1) does not allow to derive a spectral index image of the minihalo.

The extent and 1.4 GHz power of the minihalo in RXCJ1504 are in very good agreement with the size/power correlation found for other minihalos by Cassano, Gitti & Brunetti (2008).

5. Gas sloshing in the cool core

Inspection of the *Chandra* image reveals at least two subtle brightness edges in the cool core. To better illustrate these edges, we fit a symmetric elliptical β -model to the *Chandra* image and subtracted it from the real image. A smoothed residual image is shown in Fig. 3, with arrows indicating the edges and 327 MHz contours overlaid. Comparison with the temperature map shows that these are cold fronts, or contact discontinuities between two moving gas regions with different temperatures and densities (Markevitch & Vikhlinin 2007 and references therein), which indicates sloshing of the cool dense gas in the cluster core. A detailed check of their X-ray brightness profiles reveals that these edges, while relatively sharp, are not well described by a simple projected spherical gas density discontinuity, suggesting that sloshing occurs not in the plane of the sky. Cold fronts are common in the cores of otherwise relaxed clusters, and are believed to be created by sloshing of the cool, dense core gas, possibly induced by a minor merger during the past few Gyrs (e.g., Ascasibar & Markevitch 2006).

6. Discussion

Despite extensive searches, less than ten clusters are known to host a minihalo so far (Ferrari et al. 2008; Cassano, Gitti & Brunetti 2008; Govoni et al. 2009). Thus, the discovery of a new one in an extreme cool-core cluster provides useful information on their origin and the minihalo/cool-core connection.

Gitti et al. (2002) proposed that minihalos result from reacceleration of pre-existing relativistic electrons in the ICM by

¹ $S \propto \nu^{-\alpha}$, where S is the flux density at the frequency ν .

turbulence in the cooling flow. More recently, based on the observed connection between radio minihalos and X-ray cold fronts in several cool-core clusters, Mazzotta & Giacintucci (2008) proposed that, instead, the gas sloshing that creates those cold fronts may be responsible for generating the turbulence needed to reaccelerate the fossil relativistic electrons. Indeed, high-resolution numerical simulations show that sloshing can generate turbulence in the core (e.g., Fujita et al. 2004; ZuHone et al. 2010 in preparation). The radio minihalo in RXCJ1504 appears confined to the cool core region, suggesting a tight connection between the cool gas and the relativistic plasma. The X-ray cold fronts provide evidence that the gas in this cool core is also sloshing, as observed in most cool cores (Markevitch & Vikhlinin 2007). Thus, this mechanism may explain the minihalo in this cluster as well.

The acceleration timescale due to compressible turbulence is $\tau_{acc} \sim 3 \times 10^6 \left(\frac{V_l}{c_s}\right)^{-4} \frac{l/50}{c_s/1000}$ yrs, where l is the injection scale (in kpc), c_s is the sound speed and V_l is the velocity of turbulent eddies at the injection scale (Brunetti & Lazarian 2007, 2010). Consequently, $\tau_{acc} \sim \text{few } 10^8$ yrs, necessary for reacceleration of GeV electrons, can be provided by this mechanism if the energy of the turbulence, generated by core sloshing (i.e., on a scale $l \approx 50 - 100$ kpc), is $\sim 5 - 10\%$ of the thermal energy.² Recent X-ray spectral observations of A1835, a cool-core cluster with a minihalo, placed an upper limit on the energy of turbulence at $l \sim 30$ kpc scale in the cluster core of $\sim 13\%$ of the thermal energy (Sanders et al. 2010), so the required level of turbulence is allowed by current data.

In the context of the turbulent model, the high synchrotron emissivity of minihalos implies an efficient supply of seed relativistic particles to be reaccelerated in the emitting volume, which may be provided by the central AGN (e.g., Cassano et al. 2007). Because of a strong entropy decline in the cool core, sloshing does not result in cool gas spreading far outside of its equilibrium radius. Thus, fossil relativistic electrons generated by the central AGN should stay confined in the core, making the emission process efficient.

Alternative models were also proposed to explain the origin of minihalos, such as the secondary electron model (Pfrommer & Ensslin 2004), in which ultrarelativistic electrons originate from hadronic interactions of the long-lived cosmic ray protons with thermal protons. A central AGN may also supply the relativistic protons in the core. However, what would create the observed strong drop of the radio brightness at the boundary of the minihalo in this model is not clear. High-energy protons (with energies $\sim 30 - 100$ GeV) should diffuse on the 50–100 kpc scales on a short timescale, < 1 Gyr (e.g., Blasi, Gabici & Brunetti 2007). Assuming that the resulting density of cosmic ray protons is proportional to the density of thermal gas, n_{th} , the synchrotron emissivity in secondary models would scale as $j \propto n_{th}^2 B^{1+\alpha} X / (B^2 + B_{CMB}^2)$, where B is the magnetic field intensity, B_{CMB} is the equivalent field of the Cosmic Microwave Background photons and X is the ratio of the cosmic ray to thermal energy densities (Pfrommer & Ensslin 2004). For a constant B , the synchrotron brightness should then follow the X-ray brightness. However, while the radio minihalo has rather abrupt boundaries, the X-ray brightness is smooth at those radii – between $r = 30''$ and $40''$ from the centre (the interval containing

the minihalo boundary), the radio brightness declines by a factor of $\sim 7 - 8$, while the X-ray brightness decreases only by a factor ~ 1.5 (Fig. 2). In the framework of the secondary-electron model, this could be explained by a highly amplified magnetic field within the cool core (possibly as a result of gas sloshing, Keshet et al. 2010). The magnetic field strength should then decrease to $B \ll B_{CMB}$ outside the core. Faraday rotation measurements of cluster radio galaxies in systems similar to RXCJ1504 can test this possibility.

7. Conclusions

Using archival *GMRT* observations at 327 MHz and *VLA* 1.46 GHz data, we discovered a radio minihalo in RXCJ1504, with a radius of ~ 140 kpc. The host cluster is very relaxed and possesses one of the most luminous cool cores in the Universe, with 70% of the total X-ray luminosity of the cluster coming from the core region. The *Chandra* gas temperature map shows that the minihalo is confined to the cool core. We found two cold fronts in the cool core, suggesting that the core gas is sloshing. Such sloshing may generate turbulence in the core, which in turn may reaccelerate relativistic electrons, forming a minihalo. Alternatively, the minihalo can be produced by boosting of the synchrotron emission from an underlying population of electrons (e.g., secondaries) if the magnetic field is strongly amplified in the cool core. In this case, the strong drop of the radio brightness at the boundary of the cool core would imply that the magnetic field outside this region is $B \ll B_{cmb}$.

Acknowledgements. We thank the anonymous referee for constructive comments and suggestions that improved this work. We thank P. Mazzotta for useful discussions. RC and GB thank Harvard-Smithsonian Center for Astrophysics for hospitality. *GMRT* is run by the NCRA of the Tata Institute of Fundamental Research. Financial support for this work was partially provided by *Chandra* grant AR0-11017X, NASA contract NAS8-39073, by INAF under grants PRIN-INAF2007 and PRIN-INAF2008 and by ASI-INAF under grant I/088/06/0.

References

- Ascasibar, Y., & Markevitch, M. 2006, *ApJ*, 650, 102
 Bacchi, M., Ferretti, L., Giovannini, G., Govoni, F., 2003, *A&A*, 400, 465B
 Böhringer, H., Burwitz, V., Zhang, Y.-Y., et al., 2005, *ApJ*, 633, 148
 Blasi P., Gabici, S., Brunetti, G., 2007, *IJMPA*, 22, 681
 Brunetti G., & Lazarian A., 2007, *MNRAS*, 378, 245
 Brunetti G., & Lazarian A., 2010, *MNRAS*, in press (arXiv:1008.0184)
 Burns, J. O., Sulkanen, M. E., Gisler, G. R., Perley, R. A., 1992, *ApJ*, 388L, 49
 Cassano, R., Gitti, M., & Brunetti G., 2008, *A&A*, 486, 31L
 Ferrari, C., Govoni, F., Schindler, et al., 2008, *Space Science Reviews*, 134, 93
 Fujita, Y., Matsumoto, T., & Wada, K. 2004, *ApJ*, 612, L9
 Giacintucci, S., Venturi T., Macario G., et al., 2008, *A&A*, 486, 347
 Gitti, M., Brunetti, G., & Setti, G. 2002, *A&A*, 386, 456
 Gitti, M., Ferrari, C., Domainko, W., et al., 2007, *A&A*, 470L, 25G
 Govoni, F., Murgia, M., Markevitch, M., et al., 2009, *A&A*, 499, 371
 Govoni, F., & Feretti L., 2004, *IJMPD*, 13, 1549
 Keshet, U., Markevitch, M., Birnboim, Y., Loeb, A., 2010, in press (arXiv:0912.3526)
 Markevitch, M., & Vikhlinin, A., 2007, *PhR*, 443, 1
 Markevitch, M., Ponman, T. J., Nulsen, P. E. J., et al., 2000, *ApJ*, 541, 542
 Mazzotta, P., & Giacintucci, S., 2008, *ApJ*, 675, L9
 Peterson, J. R., & Fabian, A. C., 2006, *PhR*, 427, 1
 Pfrommer, C., & Ensslin, T. A., 2004, *A&A*, 413, 17
 Sanders, J. S., Fabian, A. C., Smith, R. K., Peterson, J. R., 2010, *MNRAS*, 402L, 11
 Venturi, T., Giacintucci, S., Brunetti, G., et al., 2007, *A&A* 463, 937
 Vikhlinin, A., Markevitch, M., Murray, S. S., et al., 2005, *ApJ*, 628, 655

² We note that the presence of other waves, such as Alfvén waves generated at resonant scales, may imply even larger fractions (compared to this case) of the turbulent energy available for the reacceleration of relativistic particles, making the required turbulent energy lower (e.g., Brunetti & Lazarian 2010).